

Electronic Supplementary Information

Towards sustainable manufacture of epichlorohydrin from glycerol using hydrotalcite-derived basic oxides

Giacomo M. Lari, Giorgio Pastore, Cecilia Mondelli* and Javier Pérez-Ramírez*

Institute for Chemical and Bioengineering, Department of Chemistry and Applied Biosciences, ETH Zurich, Vladimir-Prelog-Weg 1, 8093 Zurich, Switzerland.

E-mail addresses: cecilia.mondelli@chem.ethz.ch; jpr@chem.ethz.ch

Table S1. Characterisation data of the materials evaluated in the dehydrochlorination of dichloropropanol.

Sample	$V_{\text{pore}}^a / \text{cm}^3 \text{g}^{-1}$	$S_{\text{BET}}^b / \text{m}^2 \text{g}^{-1}$	$C_{\text{B}}^c / \mu\text{mol g}^{-1}$	$C_{\text{A}}^d / \mu\text{mol g}^{-1}$	$C^e / \text{wt.}\%$
MgO	0.45	482	364	6	3.0
USY	0.53	648	0	58	8.4
USY-AT	0.49	600	184	12	2.1
$\gamma\text{-Al}_2\text{O}_3$	0.50	85	5	85	5.6
MgO/USY	0.51	612	181	68	5.0
Y	0.48	680	19	221	5.2
Y-AT	0.27	406	389	161	4.1

^aVolume of N_2 adsorbed at $p/p_0 = 0.98$. ^bTotal surface area, BET method.

^cConcentration of basic sites, CO_2 -TPD. ^dConcentration of acid sites, FTIR spectroscopy of adsorbed pyridine. ^eCarbon content, elemental analysis.

Table S2. Activity and selectivity data of the materials evaluated in the dehydrochlorination of dichloropropanol.

Sample	$X_{\text{dichloropropanol}} / \%$	$S_{\text{epichlorohydrin}} / \%$	$S_{\text{chloroacetone}} / \%$	$S_{\text{others}} / \%$
MgO ^a	5.5	31.6	12.1	14.0
USY ^a	1.2	1.2	26.3	30.0
USY-AT ^a	2.2	23.4	15.5	18.8
$\gamma\text{-Al}_2\text{O}_3$ ^a	0.8	33.3	13.8	16.9
MgO/USY ^a	3.7	62.1	18.5	18.9
Y ^a	0.1	0.5	15.1	16.4
Y-AT ^a	5.0	57.2	14.6	15.6
HT2 ^a	5.9	74.3	15.7	18.0
HT2-c823 ^a	7.8	80.5	18.9	20.1
HT2 ^b	6.1	75.5	4.8	10.0
HT4 ^b	5.3	70.7	9.3	8.9
HT2-c823 ^b	7.9	79.6	3.2	7.5
HT4-c673 ^b	1.9	68.2	8.3	14.1
HT4-c823 ^b	18.2	94.8	2.7	2.6
HT4-c973 ^b	5.9	80.8	6.1	12.5

^a $T = 473 \text{ K}$, $P = 1 \text{ bar}$, $t = 0.5 \text{ h}$ and $WHSV = 6 \text{ h}^{-1}$. ^b $T = 423 \text{ K}$, $P = 1 \text{ bar}$, $t = 0.5 \text{ h}$ and $WHSV = 6 \text{ h}^{-1}$.

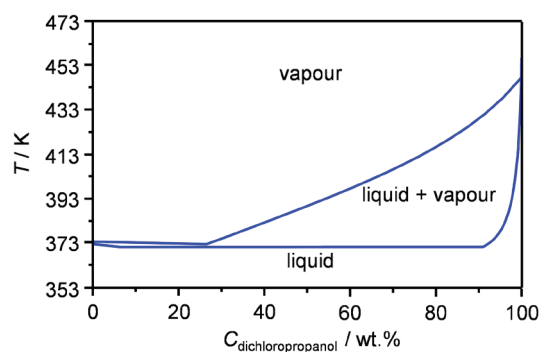


Fig. S1. Liquid-vapour equilibrium diagram for the 1,3-dichloropropanol-water mixture at 1 bar.

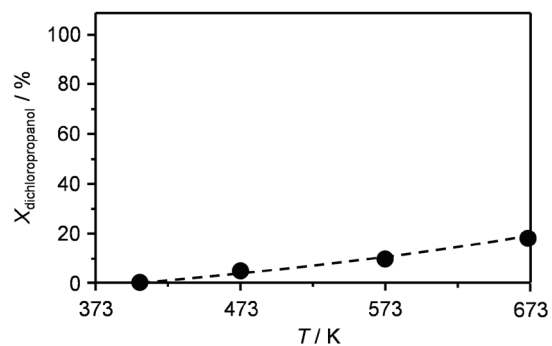


Fig. S2. Dichloropropanol conversion *versus* temperature in experiments conducted in the absence of any additional reagent at $P = 1$ bar and $WHSV = 1.2 \text{ h}^{-1}$.

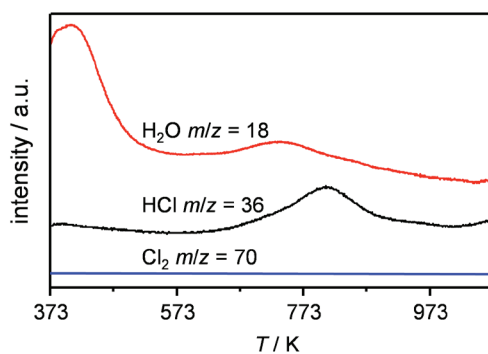


Fig. S3. Mass spectrometry analysis of the outlet gas upon the temperature-programmed oxidation (O_2 concentration in $\text{He} = 10 \text{ vol.}\%$, ramp rate = 10 K min^{-1}) of the HT4-c823 material after use in the dehydrochlorination of dichloropropanol.

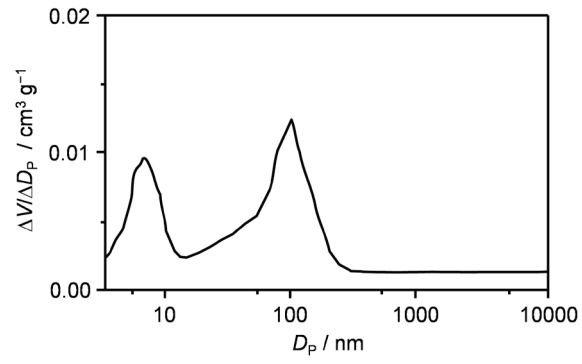


Fig. S4. Pore size distribution of HT4-c823 derived from the adsorption branch of the N_2 sorption isotherm through the application of the BJH model.